

Experimental study of low-temperature electrical radiant floor heating system

Kong Xiangqiang¹ Li Ying¹ Hu Songtao²

(¹School of Mechanical and Electronic Engineering, Shandong University of Science and Technology, Qingdao 266510, China)

(²School of Environmental and Municipal Engineering, Qingdao Technological University, Qingdao 266033, China)

Abstract: To evaluate the thermal performance of a low-temperature electrical radiant floor heating system, an experimental facility equipped with a constant temperature chamber and different specimen floors is designed and built. The heating cable is installed in the floor slab with a unit-rated power of 30 W/m. Twenty-four different schemes are worked out and tested, which include three kinds of composite floor structures and eight kinds of cable distances. The cable distances are 30, 40, 50, 60, 80, 100, 130, 150 mm. The main affective factors of the thermal performance and their influencing regularity are discussed. The experimental results show that the system has good stability and reliability, and the ratio of the radiation heat-transfer rate to the gross heat-transfer rate is greater than 50%. When the floor structure and the cable distance are fixed, the gross heat-transfer rate of the upper floor surface has a maximum value at an optimal cable distance. Under the experimental conditions in this paper, the optimal cable distance is 50 mm.

Key words: electrical radiant floor heating; floor structure; cable distance; thermal performance

Low-temperature radiant floor heating is one of the generally acknowledged ideal heating ways at home and abroad in the field of heating^[1-3]. A low-temperature electrical radiant floor heating system uses electricity as its energy source and heating cables are embedded in the floor. In the radiant floor heating system, heat is transferred by radiation and convection. This system are energy saving and comfort^[4-5].

At present, low-temperature radiant floor heating still uses central heating, a boiler room heat supply or a small-scale steam stove as the main heat sources. But on some special occasions, such as on the train, in the villa far from downtown, the heat sources mentioned above are difficult to obtain, while electric power is sufficient^[6-8]. Thus, electrical radiant floor heating systems are developed. Moreover, they can remedy the deficiencies in such aspects as automatic control and maintenance of hot water radiant floor heating systems.

This paper experimentally evaluates the thermal performance of a low-temperature electrical radiant floor heating system. The stability and reliability of the system are examined, and some regularity results are obtained.

Received 2009-11-10.

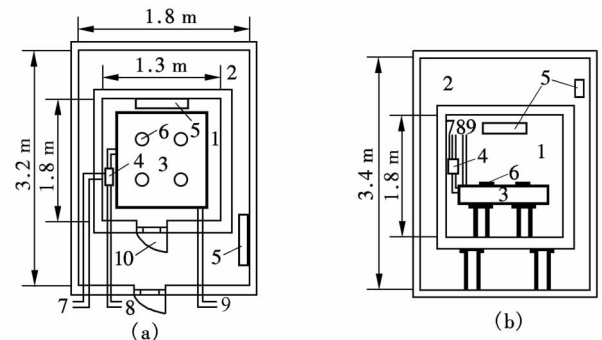
Biography: Kong Xiangqiang (1976—), male, doctor, associate professor, kxqiangly@126.com.

Citation: Kong Xiangqiang, Li Ying, Hu Songtao. Experimental study of low-temperature electrical radiant floor heating system[J]. Journal of Southeast University (English Edition), 2010, 26(2): 287 – 291.

1 Experiment

1.1 Experimental facility

This experiment is carried out in a constant temperature chamber of a size of 1.8 m × 1.3 m × 1.8 m. The chamber is placed in a temperature-controlled room, which is equipped with air conditioners to control the indoor temperature. The temperature control precision of the chamber is ± 1 °C. Fig. 1 shows the experimental facility.



1—Constant temperature chamber; 2—Temperature-controlled room; 3—Specimen floor; 4—Temperature controller; 5—Air conditioner; 6—Thermal flow meter; 7—Power cable; 8—Transformer cable; 9—Platinum resistance temperature sensor; 10—Door

Fig. 1 Experimental facility layout. (a) Plan view; (b) Front view

1.2 Floor structure and heating cable

The specimen floor used in the experiment consists of an insulating layer, a cable layer, a wood floor layer and a cover layer, as shown in Fig. 2. The insulating layer comprises a wood board layer, a fiber layer and a sheet iron layer. The cover layer comprises a carpet layer and a floor cloth layer. Heating cables are specially used in the electrical radiant floor heating system. Its unit-rated power is 30 W/m. A special-purpose temperature controller is used to limit the cable surface temperature. The heating cables are even arranged with a constant interval and the cable distances are 30, 40, 50, 60, 80, 100, 130, 150 mm. When the cable distance does not exceed 100 mm, the detector of the temperature control-

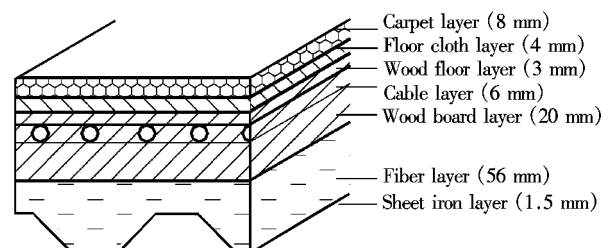


Fig. 2 Specimen floor structure

ler is installed in the center place between two adjacent cables. Otherwise, the distance between the detector and the cable is 35 mm. The electrical power is supplied from a 220 V AC transformer.

1.3 Probe arrangement and parameter measurements

The chamber temperature, the floor surface temperature, every floor layer temperature, the wall surface temperature and the cable surface temperature are measured. Besides, measurements are also made of the heat flux of each floor layer, the chamber wind velocity, the current on-off time, and the current and voltage of the heating cables. The arrangement of the temperature sensors and the heat flux sensors is shown in Fig. 3. Platinum resistance temperature sensors (Pt100, grade A, at 0 °C) are used for temperature measurements. The wind velocity is measured by a hot-bulb anemometer with a range from 0.05 to 30 m/s. The time is tested by a stopwatch. An electrical parameter measuring apparatus ($\pm 0.25\%$ accuracy) is used for electrical energy output measurements. A data acquisition logger reads and stores data about every 30 s.

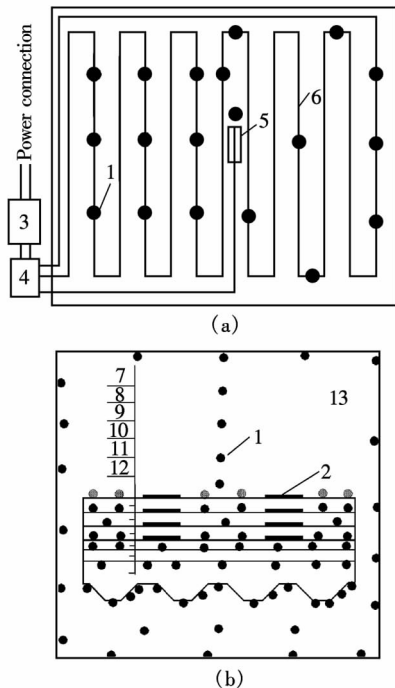


Fig. 3 Probe arrangement. (a) Cable layers; (b) Front view
1—Temperature setpoint; 2—Thermal flow meter; 3—Temperature controller; 4—Transformer; 5—Temperature detector; 6—Cable; 7—Carpet layer; 8—Floor cloth layer; 9—Wood floor layer; 10—Cable layer; 11—Wood board layer; 12—Fiber layer; 13—Constant temperature chamber

respectively.

2.1 Cable surface temperature

The influences of the floor structure and the cable distance on the cable surface temperature are depicted in Fig. 4, where the average temperature is the average time-weighted value of all setpoints on the cable during the whole run time. Under identical floor structure conditions, a longer cable distance results in a higher cable surface temperature. Under identical cable distance conditions, with the increase in the thermal resistance of the upper floor surface, both the heat dissipating capacity and the cable surface temperature decrease. Moreover, with the decrease in the thermal resistance of the upper floor surface, the influence of the cable distance on the cable surface temperature becomes greater. As seen in Fig. 4(a), when the cable distance increases from 30 to 150 mm, the cable surface temperature increases 23.8 and 15.9 °C in the case of conditions 1 and 3, respectively.

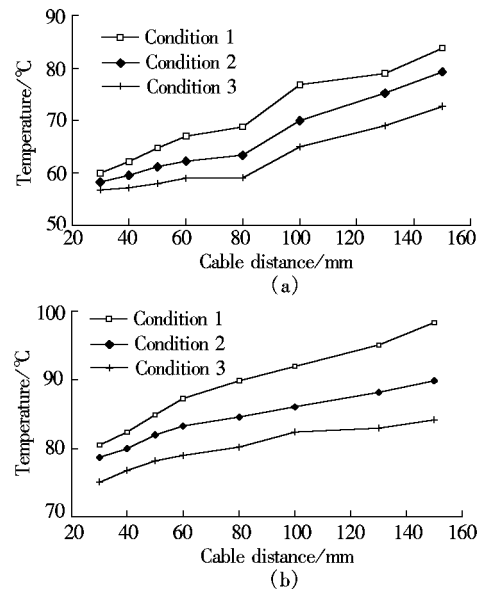


Fig. 4 Variations in cable surface temperature under different conditions. (a) Average temperature; (b) Maximum temperature

2.2 Setpoint temperature in the floor

Temperature variations versus time, floor structure and cable distance of setpoints in the floor are similar, as shown in Fig. 5. It can be seen that every setpoint temperature varies periodically, which results from the periodic fluctuations of the cable surface temperatures within an allowable range. Furthermore, when the thermal resistance of the upper floor surface and the cable distance increase, the temperature variation period becomes longer and the range of the temperature fluctuation becomes smaller. Under identical floor structure conditions, the longer the cable distance is, the less the influence of the cable distance on the setpoint temperature is. The temperature-variation reduction rate is a ratio of the temperature variation to the corresponding cable distance variation and can be calculated by

$$n = \frac{\Delta t_1 - \Delta t_2}{d_1 - d_2} \quad (1)$$

2 Results and Discussion

In the experiment, the chamber temperature is maintained at (22 ± 1) °C. Three different floor structures are measured. The first floor structure consists of a wood floor layer, a cable layer, a wood board layer, a fiber layer and a sheet iron layer. A floor cloth is added over the first floor structure, which is called the second floor structure. Then, a carpet is placed over the second floor structure, which is named the third floor structure. For convenience, three different floor structures are described as conditions 1, 2 and 3,

where Δt_1 , Δt_2 are two temperature variations, and d_1 , d_2 are their corresponding cable distances. The lower value of n represents the less influence of the cable distance on the setpoint temperature. Take condition 2 for example. When the cable distance increases from 30 to 50 mm, 50 to 100 mm, and 100 to 150 mm, the values of n are 0.050, 0.046 and 0.034 °C/mm, respectively.

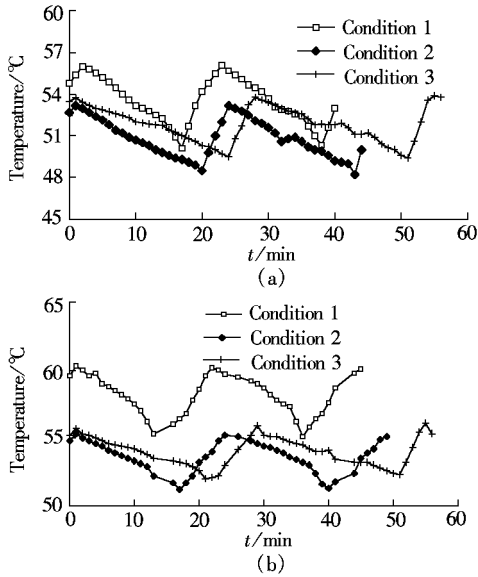


Fig. 5 Variation of setpoint temperature on upper surface of fiber layer with different cable distances. (a) 30 mm; (b) 50 mm

2.3 Convection and radiation heat transfer

For the low-temperature electrical radiant floor heating system, the heat transfer of the radiant surface comprises heat convection and radiation. So the gross heat-transfer rate is the sum of the above-mentioned two. The radiation heat-transfer rate q_r , the convection heat-transfer rate q_c , and the ratio of the radiation heat-transfer rate to the gross heat-transfer rate k_r can be calculated by

$$q_r = C_b \varepsilon \varphi (T_k^4 - T_i^4) \quad (2)$$

$$q_c = h(T_k - T_n) \quad (3)$$

$$k_r = \frac{q_r}{q} = \frac{q_r}{q_r + q_c} \quad (4)$$

where C_b is the proportionality constant with a value of $5.669 \times 10^{-8} \text{ W}/(\text{m}^2 \cdot \text{K}^4)$; ε is the emissivity with the values of 0.85, 0.87, 0.87 for the wood floor, floor cloth and carpet, respectively; φ is the view factor with a value of 1.0 in the enclosure space; T_k is the upper floor surface temperature; T_i is the inner surface temperature; T_n is the air temperature in the chamber; h is the convection heat-transfer coefficient calculated by the Nusselt number, the Prandtl number and the Reynolds number; q is the gross heat-transfer rate.

Fig. 6 shows the variations of q_r , q_c , k_r with the floor structure and the cable distance. It can be seen that the shapes of all the curves are similar for all the schemes. In other words, the influences of the floor structure and the cable distance on q_r , q_c , k_r are similar. Under identical cable distance conditions, the greater the thermal resistance of the

upper floor surface is, the smaller these four parameters are. Under identical floor structure conditions, these parameters tend to vary in terms of parabolas with an optimal cable distance of 50 mm. The ratio k_r ranges from 50.92% to 56.02%. The comparisons between the calculated and measured values of the heat-transfer rate are shown in Tab. 1, where d is the cable distance and q_m represents the measured value of the gross heat-transfer rate. A conclusion that the relative errors are within 5% can be drawn.

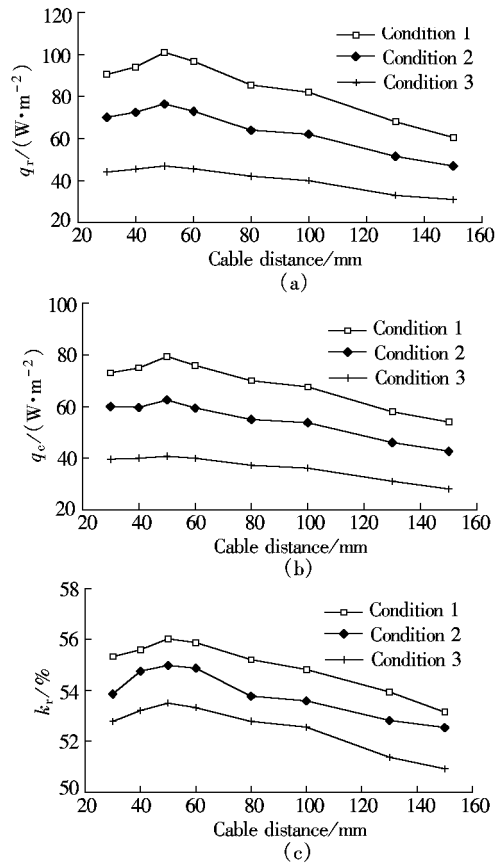


Fig. 6 Variations of q_r , q_c , k_r with floor structure and cable distance. (a) Radiation heat-transfer rate; (b) Convection heat-transfer rate; (c) Ratio of radiation heat-transfer rate to gross heat-transfer rate

Tab. 1 Comparisons between calculated and measured values of heat-transfer rate

d/mm	Floor structure	$q/(\text{W} \cdot \text{m}^{-2})$	$q_m/(\text{W} \cdot \text{m}^{-2})$	$\frac{q_m - q}{q_m} / \%$
30	Condition 1	163.6	171.8	4.77
	Condition 2	130.2	132.5	1.74
	Condition 3	83.6	86.3	3.13
50	Condition 1	180.5	189.5	4.75
	Condition 2	139.0	145.0	4.14
	Condition 3	87.6	92.0	4.78
100	Condition 1	149.7	154.4	3.04
	Condition 2	115.8	117.9	1.78
	Condition 3	76.1	78.5	3.06

2.4 Rated power and actual power of heating cable

The actual power of the heating cable is the average time-weighted power in one on-off period. The rated power and the actual power of the heating cable in the floor can be cal-

culated by

$$P = p_a l \quad (5)$$

$$P' = \frac{Px}{x+1} \quad (6)$$

where P and P' are the rated power and the actual power, respectively; p_a is the unit-rated power of the heating cable with a value of 30 W/m; l is the heating cable length; x is the on-off time ratio of one period in a steady state. Therefore, the ratio of the actual power to the rated power r_p can be calculated by

$$r_p = \frac{P'}{P} = \frac{x}{x+1} \quad (7)$$

The system with the higher value of r_p can obtain better thermal economy. Fig. 7 shows the influences of the floor structure and the cable distance on the ratio r_p . Under identical floor structure conditions, the longer the cable distance is, the higher the ratio r_p is. Under identical cable distance conditions, the greater the thermal resistance of the upper floor surface is, the lower the ratio r_p is.

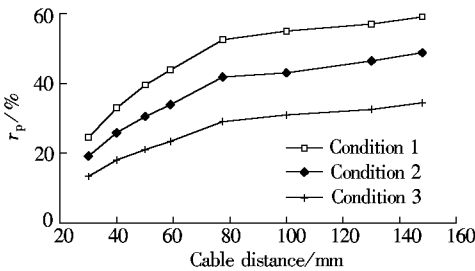


Fig. 7 Variation of r_p with floor structure and cable distance

2.5 Thermal conductivity of every floor layer

The thermal conductivity of every floor layer can be calculated by

$$\lambda = \frac{q\delta}{t_b - t_u} \quad (8)$$

where λ is the thermal conductivity; δ is the layer thickness; t_b and t_u are the below and upper surface temperatures, respectively. Based on this definition, experimental measurements can be carried out to determine the thermal conductivity of every floor layer. The results are listed in Tab. 2, where λ_w , λ_i , λ_f , λ_c are the thermal conductivities of the wood

Tab. 2 Thermal conductivity of every floor layer

Floor structure	$\lambda /$ (W·(m·°C) ⁻¹)	Cable distance/mm		
		30	50	100
Condition 1	λ_w	0.160	0.160	0.160
	λ_i	0.048	0.047	0.047
Condition 2	λ_w	0.164	0.158	0.158
	λ_f	0.083	0.080	0.080
Condition 3	λ_i	0.046	0.047	0.047
	λ_w	0.167	0.161	0.161
Condition 3	λ_f	0.084	0.082	0.082
	λ_c	0.051	0.050	0.050
	λ_i	0.046	0.047	0.047

floor layer, the insulating layer, the floor cloth layer and the carpet layer, respectively. In general, the calculated values of the thermal conductivity are similar for each layer.

3 Conclusions

The performance of the low-temperature electrical radiant floor heating system is investigated. The conclusions drawn from the experimental study are as follows:

1) The average temperature and the maximum temperature of the upper floor surface, the temperature variation in the floor, the gross heat-transfer rate of the upper floor surface, the ratio of the radiation heat-transfer rate to the gross heat-transfer rate are in inverse proportion to the thermal resistance of the upper floor surface. When the floor structure and the cable distance are fixed, the gross heat-transfer rate of the upper floor surface has a maximum with an optimal cable distance. Under the experimental conditions in this paper, the optimal cable distance is 50 mm.

2) The ratio of the radiation heat-transfer rate to the gross heat-transfer rate is greater than 0.5. The smaller the thermal resistance of the upper floor surface is, the greater the influence of the cable distance on the cable surface temperature and the gross heat-transfer rate is.

3) The temperature in the system varies periodically. The period is directly proportional to the cable distance and in inverse proportion to the thermal resistance of the upper floor surface. The system has better thermal economy with a longer cable distance and a smaller thermal resistance of the upper floor surface.

References

- [1] Hu Songtao, Yu Huili, Li Xuquan, et al. Dynamic simulation of operation of the radiant floor heating system [J]. *Heating Ventilating & Air Conditioning*, 1999, **29**(4): 15 – 17. (in Chinese)
- [2] Olesen B W. Radiant floor heating in theory and practice [J]. *ASHRAE Journal*, 2002, **44**(7): 19 – 26.
- [3] Liu Yanfeng, Liu Jiaping. Measurement and study on the heat transfer of embedded heat floor [J]. *Journal of Xi'an University of Architecture and Technology*, 2004, **36**(2): 176 – 178. (in Chinese)
- [4] Sattari S, Farhanieh B. A parametric study on radiant floor heating system performance [J]. *Renewable Energy*, 2006, **31**(10): 1617 – 1626.
- [5] Zhao Wei, Zhang Yufeng, Deng Na, et al. Experimental investigation on the performance of solar-thermosyphon embedded radiant floor heating system [J]. *Acta Energiae Solaris Sinica*, 2008, **29**(6): 637 – 643. (in Chinese)
- [6] Chen Haibo, Huang Haizhen, Lü Quantao. Calculation of radiant heat from low-temperature hot water floor [J]. *Journal of Jinlin University: Engineering and Technology Edition*, 2005, **35**(2): 136 – 140. (in Chinese)
- [7] Zhang Dongliang, Wang Zijie, Zhang Xu. Thermal performance of dye-type floor panel heating system [J]. *Heating Ventilating & Air Conditioning*, 2009, **39**(8): 51 – 56. (in Chinese)
- [8] Lin Kunping, Zhang Yinping, Xu Xu, et al. Experimental study of under-floor electric heating system with shape-stabilized PCM [J]. *Energy and Buildings*, 2005, **37**(3): 215 – 220.

低温电地板辐射供暖系统的实验研究

孔祥强¹ 李 璘¹ 胡松涛²

(¹ 山东科技大学机械电子工程学院, 青岛 266510)

(² 青岛理工大学环境与市政工程学院, 青岛 266033)

摘要:为了评价低温电地板辐射供暖系统的热力性能,设计并构建了一个由恒温小室和不同结构地板组成的实验装置.发热电缆均匀分布在地板层内,额定发热功率为 30 W/m.由 3 种不同复合地板结构和 8 种不同的导线间距组合成 24 种实验方案,分别进行测试,其中导线间距分别为 30,40,50,60,80,100,130,150 mm.分析了影响电地板辐射供暖系统热力性能的主要因素及其影响规律.实验结果表明,该系统具有良好的稳定性和可靠性,地板供暖辐射换热量约占总换热量的 50% 以上.当地板结构相同且感温探头所处位置不变时,存在一个使地板上表面散热量最大的最佳导线间距,实验工况下的最佳导线间距为 50 mm.

关键词:电地板辐射供暖;地板结构;导线间距;热力性能

中图分类号:TU832